ULTRASONIC IMAGES OF FLOW REGIONS IN A WAVE TANK

Kaneko, Arata
Research Institute for Applied Mechanics, Kyushu University : Associate Professor

Honji, Hiroyuki
Research Institute for Applied Mechanics, Kyushu University : Professor

https://doi.org/10.5109/6781010

出版情報：Reports of Research Institute for Applied Mechanics. 31 (98), pp.75-84, 1984-02. 九州大学応用力学研究所
バージョン：
権利関係：

Reports of Research Institute for Applied Mechanics
Vol. XXXI, No. 98, 1984

ULTRASONIC IMAGES OF FLOW REGIONS IN A WAVE TANK

By Arata KANEKO* and Hiroyuki HONJI†

The backscattering pattern of ultrasonic waves from jet and wake flow regions in a water tank has been imaged on the color CRT display of the echo sounding device with a 200 kHz disk-type transducer. This technique may be used to measure various flow regions in the ocean.

Key words : Water-tank experiment, Echo sounding device, Ultrasonic image, Flow region.

1. Introduction

Sound waves which can propagate over the long distance in water have been used as a tool to detect the internal structure of the ocean[1)-6)]. In the ocean, there are many causes to scatter sound waves such as ocean currents, vortices, turbulence, internal waves and suspended particles[7)-9)]. Although many attempts to detect internal waves and suspended particles by the acoustic backscattering technique have been made, acoustic detection of flow regions in a homogeneous fluid still remains as a next problem.

The purpose of this paper is to image on the color CRT display of an echo sounding device the backcattering pattern of ultrasonic waves from flow regions induced in a water tank. Jet and wake flow regions are tested.

2. Instrumentation[10)] and water tank

Measurements were made by means of the echo sounding device (Koden Electronics Co. Ltd., ECHO SOUNDER CVS-8800) which can image on a color CRT display the backscattering pattern of ultrasonic waves from a target in water. A block diagram of the electronics system is sketched in Fig. 1. The acoustic signal of time interval 0.7 ms was released from a 200 kHz piezoelectric disk-type transducer at 224 times a second. The acoustic pressure level of the signal at 1 m from the transducer was adjusted in a small range near 3.2×10^4

* Associate Professor, Research Institute for Applied Mechanics, Kyushu University, Kasugashi, Fukuoka 816, Japan.
† Professor, Research Institute for Applied Mechanics, Kyushu University, Kasugashi, Fukuoka 816, Japan.

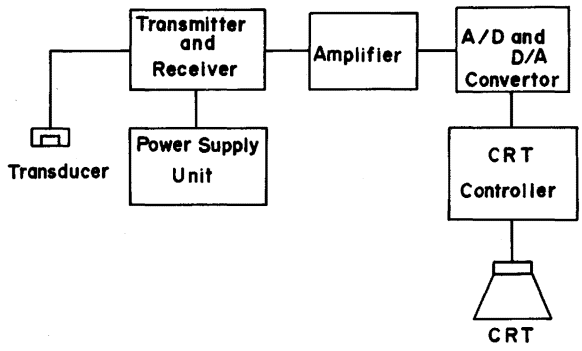

Fig. 1. Block diagram of the electronics system.

Pa. A logarithmic plot of beam pattern of the transducer is illustrated in Fig. 2. The first and second sidelobe in the beam pattern have directions of 8° and 25° and the level of -15.3 *dB* and -22.1 *dB*, respectively, from the beam center. The level (*dB*) of acoustic intensity (I) in any directions is calculated using the maximum intensity (I_o) at the beam center from the following equation

$$dB = 10 \log_{10} \frac{I}{I_o} \tag{1}$$

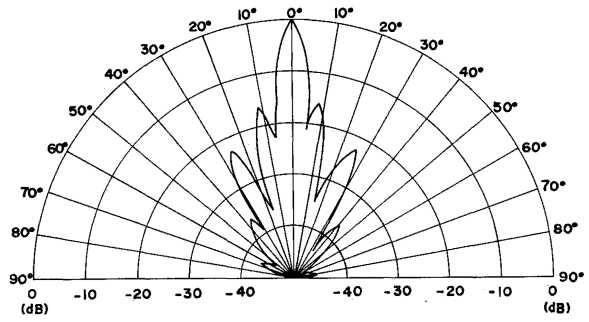

Fig. 2. Logarithmic plot of the beam pattern of a disk-type transducer.

The acoustic signal backscattered from the target was received by the same transducer before the release of a next source sigal. It should be noted that the acoustic pressure received at an instant is the summation of pressure from the traget at the same distance from the transducer. The voltage generated by the received signal through piezoelectricity was amplified to make a clear image of the target on the color display. Eight kinds of colors ranging from violet to red was selected according to the level of voltage as indicated in Table 1. Images

Table 1 The range of voltage for each color

Voltage (V)	0.0— 0.6	0.6— 1.3	1.3— 2.2	2.2— 3.5	3.5— 4.8	4.8— 6.4	6.4— 8.4	8.4<
Color	violet	blue	white	light blue	green	yellow	orange	red

on the CRT display were photographed by means of a 35 mm camera. Experiments on the transmission of acoustic becams were carried out in a water tank 70 m long, 8 m wide and 3.5 m deep. The schematic diagram of experimental set-up is presented in Fig. 3. The depth of water was 3 m. A disk-type transducer was placed at 1 m from one side wall and at a middle depth. The center line of acoustic beam released from the transducer was directid to become parallel to the bottom wall and perpendicular to the other side wall. For convenience' sake, we shall make use of the Cartesian coordinates (x, y, z) as shown in Fig. 3. The water temperature and the turbidity concentration in the tank were respectively 16.4°C and 0.7 mg/l over the whole depth.

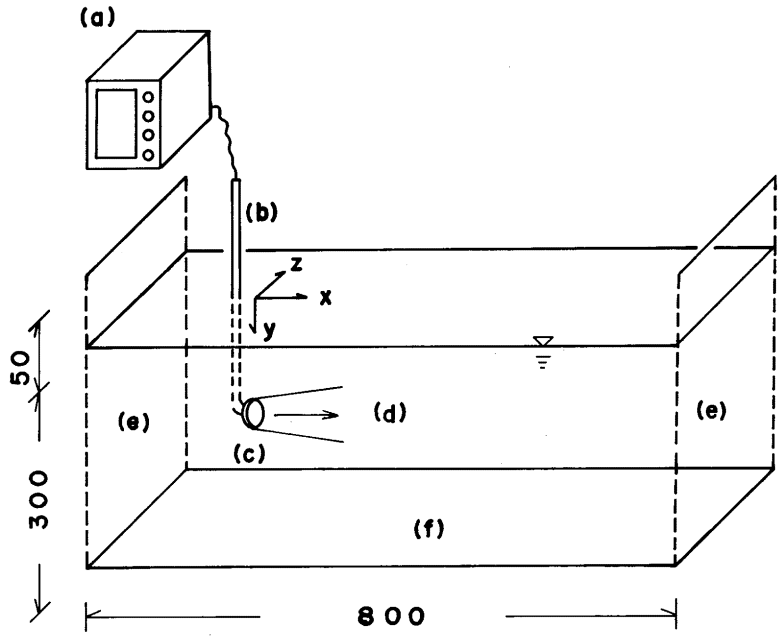

Fig. 3. Schematic diagram (bird's eye view) of the experimental set-up (dimension in cm).
(a) Color display (b) Support (c) Transducer
(d) Acoustic beam (e) Side wall (f) Bottom wall

3. Results and discussion

Let us first examine the fundamental characteristics of the echo sounding device. Five nylon threads of 0.04 cm in diameter were arrayed at intervals of 1 m in the x direction at the positions seen in Fig. 4. Figure 5 shows the ultrasonic image of the nylon-thread array suspended in water. A scale on the right-hand side of the display indicates the distance from the transducer in the unit of m. Eight kinds of colors used in imaging are arrayed vertically at the left-hand edge of the display. The transducer is put in the state to receive a backscattering signal while the reverberation of a source signal still remains. The red zone visible at $0 < x < 1.5$ m is generated by such a effect so that the target in this region cannot be detected. The reflection of ultrasonic waves by the distant side wall is imaged with a thick red zone at $x = 7$m. The present-time image of targets between $x = 1.5$ and 7 m appears first at the right-hand edge of the display and move leftwards at a speed of 0.23 cm/s as time proceeds. Since the width of the display is 17.3 cm, the image for about 75 s remains on the display. A series of thin red zones seen at $x = 2,3,4,5$ and 6 m are the images of the nylon-thread array. The width of each red zone is almost the same. This fact means that the transmission loss of ultrasonic waves in this distance is sufficiently small.

A group of glass beads of total weight 0.5 g was dropped into the water so that they fell freely along the line $x = 5$ m in the plane $z = 0$. The mean diameter (D) and the density (ρ_s) of glass beads used were 0.028 cm and 2.43 g/cm^3, respectively. Figure 6a shows the image before glass beads are dropped into water. The weak scattering zones at 3.5 m $< x <$ 5.5 m may relate to the positions where the second sidelobe in the beam pattern crosses a water surface or a bottom wall. Figure 6b shows the image at 67 s after the start of fall of glass beads. The group of glass beads falling is detected as a row of white spots at $x = 5$ m. The length of the row indicates the time (37 s) during which the group of glass beads passes throgh the main part of acoustic beam.

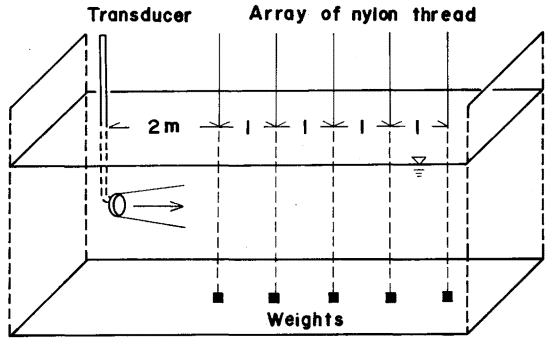

Fig. 4. Nylon-thread test.

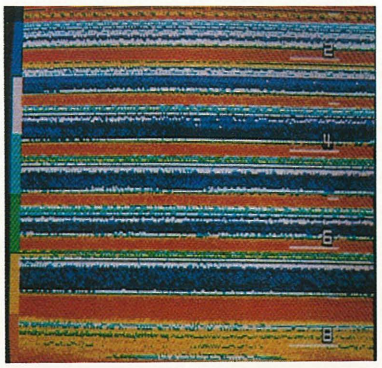

Fig. 5. The ultrasonic image of a nylon-thread array.

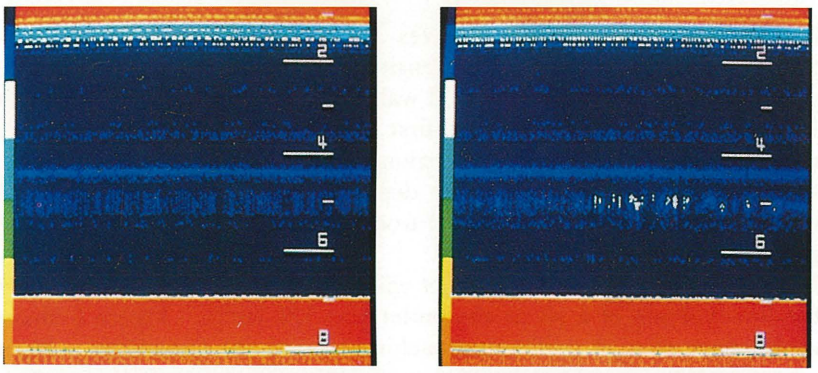

Fig. 6. The ultrasonic images of a group of glass beads falling freely in water. Time measured from the start of falling is denoted by t. (a) $t = 0$ s (b) $t = 67$ s

Considering that the grouped bead reached the beam center ($y = 150$ cm) at 42 s, we can estimate the fall velocity (w) of the beads as 3.6 cm/s. This value is in good agreement with 3.3 cm/s calculated by Rubey's formula[11]

$$w^2 = \frac{4}{3}\frac{gD}{C_D}\frac{\rho_s - \rho_f}{\rho_f}$$

$$C_D = 24/R_e + 2 \qquad (2)$$

$$R_e = wD/\nu$$

where C_D and g are respectively the drag coefficient and the acceleration due to gravity, and ρ_f *and* ν the density and the kinematic viscosity of a fluid.

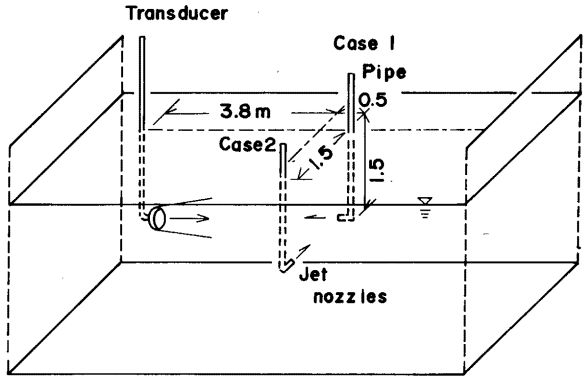

Fig. 7. Circular jet experiment.

It is well known that sound waves are refracted by the shear flow in a homogeneous fluid as well as by the density-stratified region[12]. The problem of scattering of sound waves from jet and wake flow regions with organized motion may be more complicated. We shall first examine the backscattering pattern of ultrasonic waves from circular jet regions. A nozzle of 1 cm diameter was placed horizontally at the same water depth as that of the transducer. Water in the tank was used as a fluid ejected from the nozzle. Two cases as sketched in Fig. 7 were tested.

In case 1, the axis of a circular jet coincided with that of an acoustic beam and the flow volume of a jet at the outlet was 121 cm^3/s. Figure 8 shows the ultrasonic image of a jet region approaching toward the transducer. Figure 8a is the image before the water jet is ejected. An intense scattering zone due to the pipe inserted in water is visible at $x = 4.2$ m. Figures 8b-d are respectively the images at 31 s, 66 s and 106 s after the ejection of a jet started. The process in which the front of a jet region moves to the transducer can clearly be understood from these figures. The movement of the front makes a parabora on the display and the slope of its tangent means the moving velocity of the front at each place. The velocity slows down successively as the transducer is approached. The distance from the nozzle to the front of a jet is denoted by x' and the time after the start of jet ejection by t. According to the theory of a turbulent circular jet[13], the moving velocity (u_m) of a front may obey the following equation

$$u_m = \frac{c}{x'} \tag{3}$$

where c stands for a constant with dimension in cm^2/s. Substituting $u_m = dx'/dt$ into eq. 3 and integrating the resulting equation with respect to, t, we obtain

$$x' = \sqrt{2ct} \tag{4}$$

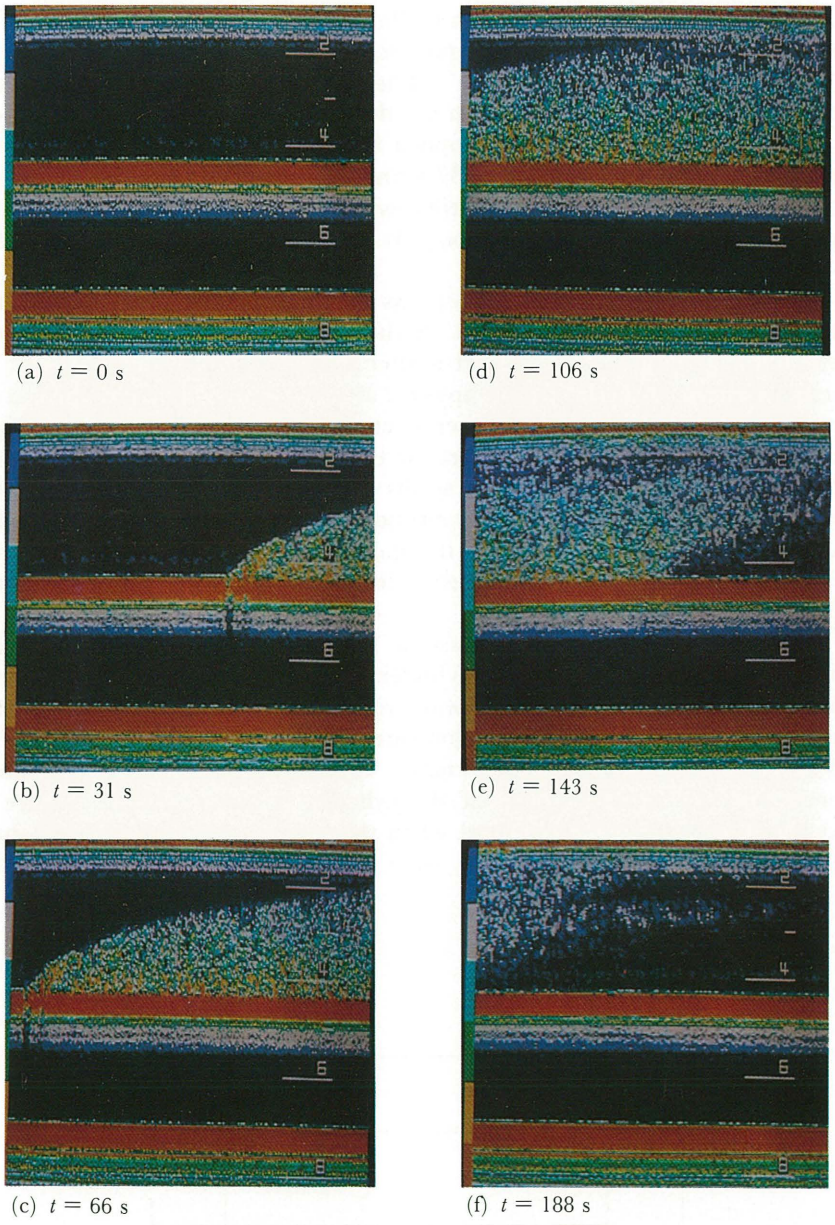

(a) $t = 0$ s (d) $t = 106$ s

(b) $t = 31$ s (e) $t = 143$ s

(c) $t = 66$ s (f) $t = 188$ s

Fig. 8. Circular jet with the same axis as that of acoustic beam. Time measured from the start of jet ejection is denoted by t. The ejection was stopped at $t = 106$ s.

which gives the position of a front at t. Putting $c = 450$ cm^2/s, eq. 4 has a best fit with the parabora of Fig. 8c. Figure 8c also shows that the level of scattering in the jet region reduces with x'. The decrease of flow velocity in the x' direction may be responsible for such a reduction of scattering level. The ejection of water from the nozzle was stopped at 106 s. Figures 8e and f show the ultrasonic images of flow regions at 37 s and 82 s, respectively, after the stop of ejection. The region where no scattering exists first appears near the nozzle and rapidly propagates in the x' direction. It took more than one minute for the flow region to decay completely.

In case 2, the axis of a circulr jet was perpendicular to that of an acoustic beam and the flow volume of a jet at the outlet was 131 cm^3/s. Figure 9a shows the image of a jet region at 41 a after the ejection of water started. The scattering pattern of the jet regoin appears at $x = 3.8$ m. The red zone at $x = 4.2$ m was generated by a pipe for jet ejection. Figure 9b shows the image at 88 s. The level of scattering is highest at the center of a jet and decreases with the distance from the jet center. It seems that the level of scattering relates to the magnitude of flow velocity. The ejection of water from the nozzle was stopped at this stage. Figure 9c shows the image of flow regions at 83 s after the stop of ejection. The level of scattering decreases successiively in parallel with the decay of flow regions.

We shall next examine the ultrasonic image of a wake flow region formed behind an obstacle. The circular cylinder of 9 cm in diameter and 17 cm in height was used as an obstacle. A wake region was generated by lifting-up the cylinder suspended in water by a nylon thread as sketched in Fig. 10. The upward speed of the cylinder was 46 cm/s. The Reynolds number based on the diameter and the upward speed of the cylinder is about 37600. Figure 11a shows the ultrasonic image obtained when the circular cylinder was still on the bottom wall. An intense scattering zone due to the cylinder and the thread

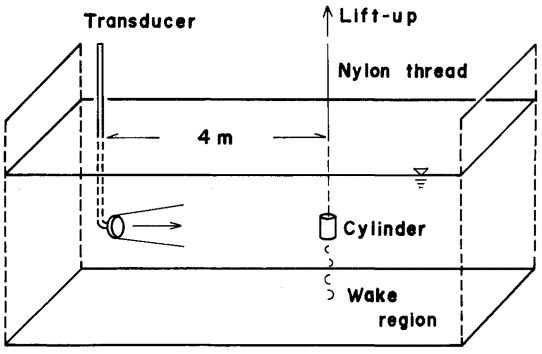

Fig. 10. Wake flow experiment.

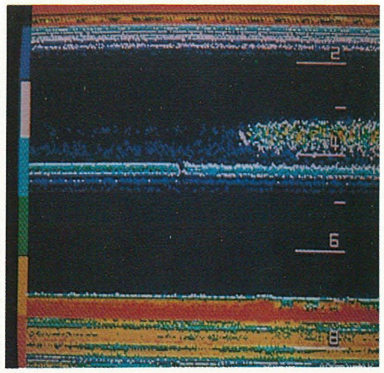

(a) $t = 41$ s

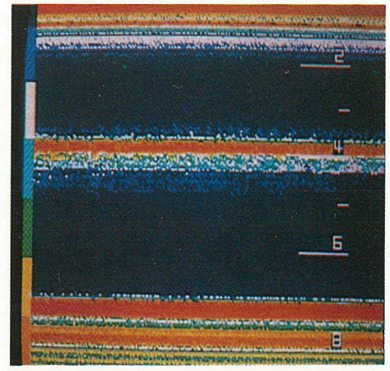

(a) $t = 0$ s

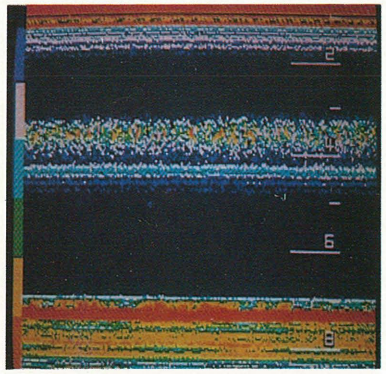

(b) $t = 88$ s

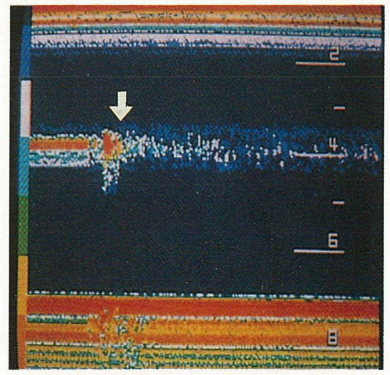

(b) $t = 54$ s

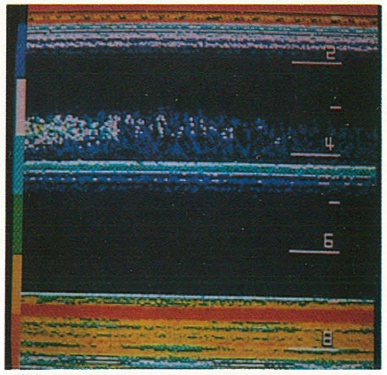

(c) $t = 171$ s

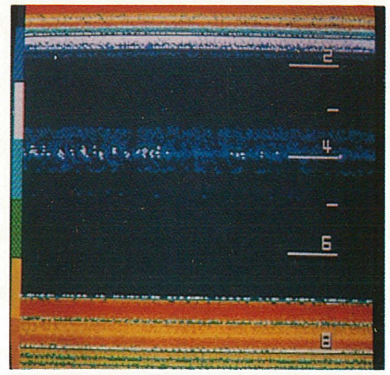

(c) $t = 123$ s

Fig. 9. Circular jet with the axis perpendicular to that of acoustic beam. Time measured from the start of jet ejection is denoted by t. The ejection was stopped at $t = 88$ s.

Fig. 11. Wake flow behind a circular cylinder lifted-up along its axis in water. Time measured from the start of lifting-up is denoted by t. The circular cylinder is initially put on the bottom wall.

appears at $x = 4$ m. Figures 11b and c show the images of a wake regoin left in water after the cylinder went out above the water surface. The position of disappearance of the cylinder in water is marked with a white arrow in Fig. 11b. Figures 11b and c are the images at 47 s and 116 s, respectively, after the disappearance of the cylinder. The wake regoin decayed monotonously with time and the decay process was analogous to that of the jet region seen in Fig. 9c.

This acoustic technique may also be applicable to more complicated flow regions in the ocean.

Acknowledgments

The authors wish to express their sincere thanks to the staff of the ocean environmental research division for encouragement and help. We also thank Messrs. Y. Shiraishi, M. Inada and Y. Namidome for technical assistance.

References

1) Vastano, A. C. & Owens, G. E.: *On the Acoustic Characteristics of a Gulf Stream Cyclonic Ring,* J. Phys. Oceanogr. **3** (1973) 470.
2) Orr, M. H. & Hess, F. R.: *Remote Acoustic Monitoring of Natural Suspensate Distributions, Active Suspensate Resuspension, and Slope / Shelf Water Intrusions,* J. Geophys. Res. **83** (1978) 4062.
3) Farmer, D. M. & Smith, J. D.: *Tidal Interaction of Stratified Flow With a Sill in a Knight Inlet,* Deep-Sea Res. **27A** (1980) 239.
4) Thorpe, S. A. & Hall, A. J.: *The Characteristics of Breaking Waves, Bubble Clouds, and Near-Surface Currents Observed Using Side-Scan Sonar,* Continental Shelf Res. **1** (1983) 353.
5) Crocker, T. R.: *Near-Surface Doppler Sonar Measurements in the Indian Ocean,* Deep-Sea Res. **30A** (1983) 449.
6) Pinkle, R.: *Doppler Sonar Observations of Internal Waves: Wave-Field Structure,* J. Phys. Oceangr. **13** (1983) 804.
7) Urick, R. J.: *Principles of Underwater Sound,* (McGraw-Hill, New York, 1975).
8) Flatté, S. M. (ed.): *Sound Transmission Through a Fluctuating Ocean,* (Cambr. Univ. Press, Cambridge, 1979) p. 299.
9) Brekhovskikh, L. & Lysanov, Y.: *Fundamentals of Ocean Acoustics,* (Springer, Berlin, 1982) p. 250.
10) Ristic, V. M.: *Principles of Acoustic Devices,* (John Wiley, New York, 1983) p. 359.
11) Raudkivi, A. J.: *Loose Boundary Hydraulics,* 2nd ed. (Pergamon, Oxford, 1978) p. 397.
12) Lighthill, J.: *Waves in Fluids,* (Cambr. Univ. Press, Cambridge, 1978) p. 504.
13) Schlichting, H.: *Boundary-Layer Theory,* 6th ed. (McGraw-Hill, New York, 1968) p. 747.

(Received November 30, 1983)